

# EADReg: Probabilistic Correspondence Generation with Efficient Autoregressive Diffusion Model for Outdoor Point Cloud Registration

Linrui Gong  
Shanghai Jiao  
ttrr2021@sjtu.edu.cn

Jiuming Liu  
Shanghai Jiao Tong University  
liujiuming@sjtu.edu.cn

Junyi Ma  
Shanghai Jiao Tong University  
junyi.ma@sjtu.edu.cn

Lihao Liu  
University of Cambridge  
11610@cam.ac.uk

Yaonan Wang  
Hunan University  
yaonan@hnu.edu.cn

Hesheng Wang\*  
Shanghai Jiao Tong University  
wanghesheng@sjtu.edu.cn

## Abstract

Diffusion models have shown the great potential in the point cloud registration (PCR) task, especially for enhancing the robustness to challenging cases. However, existing diffusion-based PCR methods primarily focus on instance-level scenarios and struggle with outdoor LiDAR points, where the sparsity, irregularity, and huge point scale inherent in LiDAR points pose challenges to establishing dense global point-to-point correspondences. To address this issue, we propose a novel framework named EADReg for efficient and robust registration of LiDAR point clouds based on autoregressive diffusion models. EADReg follows a coarse-to-fine registration paradigm. In the coarse stage, we employ a Bi-directional Gaussian Mixture Model (BGMM) to reject outlier points and obtain purified point cloud pairs. BGMM establishes correspondences between the Gaussian Mixture Models (GMMs) from the source and target frames, enabling reliable coarse registration based on filtered features and geometric information. In the fine stage, we treat diffusion-based PCR as an autoregressive process to generate robust point correspondences, which are then iteratively refined on upper layers. Despite common criticisms of diffusion-based methods regarding inference speed, EADReg achieves runtime comparable to convolutional-based methods. Extensive experiments on the KITTI and NuScenes benchmark datasets highlight the state-of-the-art performance of our proposed method. Codes will be released upon publication.

## 1. Introduction

Point cloud registration (PCR) in outdoor environments is a fundamental task, which aims to compute the 6-DOF rigid

\*Corresponding Author

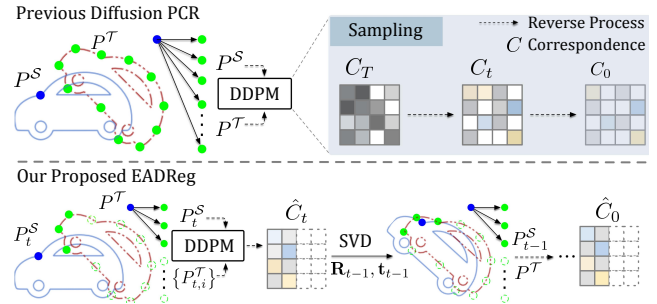


Figure 1. **Comparison with previous Diffusion PCR methods.** Previous diffusion-based PCR methods directly generate global dense point-to-point (P2P) correspondences  $C_t \in \mathbb{R}^{N^S \times N^T}$ , resulting in high training costs. In contrast, our proposed EADReg predicts correspondences within the top-K nearest neighbors of the source points  $\hat{C} \in \mathbb{R}^{N^S \times K}$ , leveraging reliable coarse registration. Besides, We integrate an autoregressive framework into the reverse process to better suit PCR tasks.

transformation between two LiDAR frames. It is essential to various downstream applications, such as global localization [11, 44, 50, 60], SLAM [4, 18, 25], navigation and auto-driving applications [10, 26, 31, 34, 35, 42, 44]. The formal procedure for PCR involves extracting reliable point features using hand-crafted or learning-based methods, introducing alignment algorithms to establish point-to-point (P2P) correspondences, and finally calculating the transformation parameters via singular value decomposition (SVD).

Establishing accurate P2P correspondences is a key issue in PCR [7, 33, 47, 69]. Recent methods have concentrated on enhancing the reliability of point correspondences. Geo-Transformer [47] improves the correspondence establishment by introducing the geometric transformer into PCR tasks. DiffusionPCR [7] constructs a powerful transformer feature extraction module to ensure high-quality correspon-

dence generation. RoReg [55] introduces oriented descriptors with both rotation equivariance and invariance to enhance correspondences. However, due to noisy inputs and unreliable feature correlations, previous regression-based methods still struggle to find accurate P2P correspondences

Distinct from regression methods, we resort to diffusion models in this paper to improve the robustness for P2P estimation with a correspondence-generation manner. Recently, Denoising Diffusion Probabilistic Models (DDPMs) have demonstrated a strong ability in domains such as image and video generation, segmentation, image matching, and motion prediction [20, 23, 37, 43, 65], which generate realistic predictions from standard Gaussian noise. Inspired by these advancements, Some studies attempt to extend diffusion models into point cloud registration [7, 24, 48, 58] for accurate dense correspondence generation and transformation matrix regression. DiffusionPCR [7] uses diffusion to directly regress transformation parameters, while Diff-PCR [58] employs optimal transport for supervision to enhance correspondence reliability. However, few of these methods generalize well to outdoor scenarios. The challenges primarily arise from the huge point scale of LiDAR points, where establishing the dense correspondences for outdoor LiDAR commonly leads to unaffordable increasing computational costs, hindering the real-world applications.

To address these challenges, we propose a novel probabilistic method named **Efficient Autogressive Diffusion** for outdoor LiDAR Point Cloud **Registration (EADReg)**, which combines GMM-based outlier correspondence rejection in the coarse layer with the diffusion-based robust point-to-point correspondence estimation in the refinement layers. Specifically, we adopt a coarse-to-fine registration paradigm, downsampling the point cloud pairs through hierarchical networks [39]. To perform reliable coarse registration, it’s crucial to effectively remove noisy points. Unlike previous methods that introduce extra parameters to identify outliers [5, 6, 61], we design a training-free **Bi-directional Gaussian Mixture Models Outlier Removal module (BGMM)** to reject outliers. By filtering the outlier GMM distributions and their associated points, we can perform reliable coarse registration based on the features and geometric information of the remaining points.

Moreover, inspired by diffusion-based temporal motion prediction methods [1, 51, 53], we re-think diffusion-based PCR as an autoregressive process. For inference, the diffusion model generates a robust point correspondence matrix between adjacent sampling steps, which are decomposed into translation and rotation components to warp the input source points, forming the source points for the next step. By learning the posterior distribution of ground truth correspondence matrixes, our model iteratively refines the registration, with each transformation preserved in a history buffer. The final result is derived from the sequential prod-

uct of all transformations. Our contributions are as follows:

- We propose EADReg, a novel outdoor PCR method that integrates Bi-directional Gaussian Mixture Models (BGMMs) to filter out outliers and treats single-frame PCR as a sequential registration process within an autoregressive diffusion paradigm, ensuring strong robustness to perturbations in outdoor LiDAR point clouds.
- Benefiting from reliable coarse registration, EADReg focuses on the top-K nearest neighbors of the source points to find true correspondences, significantly reducing computational complexity and memory usage. This results in computational speed comparable to convolution-based methods while maintaining high precision.
- Extensive experiments on the KITTI and NuScenes benchmark datasets demonstrate that our method outperforms state-of-the-art approaches, showcasing convincing performance in challenging outdoor scenarios.

## 2. Related Work

PCR is a fundamental research task in 3D computer vision field. In this section, we respectively discuss prior *Learning-based PCR Methods*, *GMMs-based PCR Methods*, and *Diffusion-based PCR Methods*.

**Learning-based PCR Methods.** Traditional methods like Iterative Closest Point (ICP) [2] and RANSAC [13] are designed for the registration task. However, these methods require either favorable initial transformations or point-level correspondences. With the advent of deep learning techniques, learning-based methods [29, 36, 39, 47] have achieved significant success in the PCR task. Relying on powerful backbones like PointNet [45], KPConv [52], and Point TransFormer [66], these methods generally downsample the original point cloud into superpoints and generate associated features with informative information. Subsequently, the transformation can be derived by constructing accurate point-to-point (P2P) correspondences. Unlike indoor and object-level registration, outdoor point clouds scanned from LiDAR sensors typically exhibit higher sparsity and larger point magnitude, leading to more challenging registration issues. To address these challenges, specific designs have been made to ease the difficulty and reduce the network burden during training. HRegNet [39] and RegFormer [32] introduce a coarse-to-fine framework to perform registration hierarchically, which accommodates the training process with increasing point magnitudes. However, employing prevalent powerful Transformer architecture to extract representative features is inevitable leading to slow convergence and significant memory usage.

**GMMs-based PCR Methods.** Unlike point-level registration, GMMs-based PCR methods model point clouds via the Expectation-Maximization (EM) optimization algorithm into several clusters and perform alignment based on the modeling results. DeepGMR [64] estimates transfor-

mations by minimizing the divergence between GMMs of source and target point clouds. JRMPC [12] and Filter-Reg [14] fit point clouds to GMM distributions using Maximum Likelihood Estimation (MLE). However, due to the sparsity of outdoor LiDAR point cloud scenes, the characteristics of different distributions can be inconspicuous, leading to degraded registration results on outdoor datasets. G3Reg [46] introduces a variant of GMMs named Gaussian Ellipsoid Model with Pyramid framework to improve the outdoor LiDAR performance. Considering the drawbacks of GMMs, directly utilizing GMMs for outdoor LiDAR registration can be challenging. Hence, we take advantage of the modeling ability of GMMs and reject the points contained in the outlier GMMs. Eliminating the misleading effect caused by the outliers, the coarse registration can be easily conducted with the source and target points.

**Diffusion-based PCR Methods.** The generative model DDPMs [19] has made great development in many fields, including image and semantic matching [17, 41, 43], human motion estimation [1, 51, 53], camera pose estimation [56], etc. Recently, A few attempts [24, 48, 58] have been made to extend diffusion into point cloud registration (PCR) for accurate dense correspondence generation and translation matrix regression. DiffusionPCR [7] introduces diffusion as a reliable regressor which directly generates the transformation parameters through the extracted representative point features. SE3Diff [24] demonstrate that the accurate diffusion process towards transformation matrices should be strictly constrained by the Lie algebra regulation. Diff-PCR [58] utilizes OT to construct the global P2P correspondence ground truth as supervision and forces the diffusion to generate the reliable correspondence. These methods show that DDPMs are capable of dealing with the instance-level PCR tasks. However due to the sparsity and low discriminability of LiDAR point cloud characteristics, these methods can hardly generalize towards outdoor LiDAR scenarios. Autoregressive diffusion (AR) [16, 21, 53, 59] presents fascinating characteristics topological nodes and sequential motion generation, Inspired by this observation, EADReg converts the single frame PCR into a sequence modeling task and achieves superior registration performance through AR’s inference paradigm in the outdoor scenarios.

### 3. EADReg

#### 3.1. Network Pipeline

Establishing dense point-to-point correspondence is infeasible and computationally-denied due to the huge point scales in outdoor scenes. Therefore, EADReg adopts a coarse-to-fine paradigm, which firstly utilizes the descriptor-detector backbone [39] to hierarchically down-sample the point clouds and extract the corresponding multi-scale features. Specifically, given source and target point clouds  $P^S, P^T \in$

$\mathbb{R}^{N \times 3}$ , the detector utilizes Weighted Furthest Point Sampling (WFPS) [68] to downsample the point clouds to different scales of superpoints  $P_l \in \mathbb{R}^{N_l \times 3}$ , then the descriptor module extracts their corresponding descriptor  $D_l \in \mathbb{R}^{N_l \times C}$  and uncertainty values  $U_l \in \mathbb{R}^{N_l}$ , where  $N_l, C_l$  are the number of superpoint and channel, the corner mark  $l \in \{c, f\}$  indicates the coarse and fine registration stage. The details of the detector-descriptor backbone will be provided in supplementary material.

Since the PCR task has a demand for high inference speed, the prediction networks  $\mathcal{F}_c$  we used in the coarse and  $\mathcal{F}_f$  in fine stage are similar and only constitute with several light-weight CBR (Convolution, Batch Normalization and ReLU) modules, the details of  $\mathcal{F}_f$  is shown in the bottom of Fig. 2, the forward process will be discussed in the Sec. 3.2 and Sec. 3.3.

#### 3.2. Bi-directional GMMs for Outlier Removal

In previous works, GMMs are widely used to perform registration between point cloud pairs [12, 14, 46, 64]. Specifically, they first model the point cloud pairs with GMMs, then use the Expectation Maximization (EM) algorithm [9] to estimate the real transformation between GMM clusters, which alternates between Expectation step and Maximization step for several iterations.

However, the estimation performance of the GMMs-based registration method heavily relies on the modeling quality of GMMs. Due to the presence of noise and outliers in outdoor scenes, performing registration between the GMMs group of the LiDAR point cloud pairs will lead to the poor performance. In this work, instead of leveraging GMMs as a predictor to estimate the transformation matrix, we adopt it as an outlier-rejection module based on the geometric features of GMMs. Unlike previous learning-based outlier prediction methods [5, 6, 61], we introduce no extra parameters leading to high efficiency. Specifically, GMMs are first used to establish a multi-modal probability distribution over 3D space which can be represented as a weighted sum of  $J$  Gaussian distributions as follows:

$$p(\mathbf{x} | \Theta) := \sum_{j=1}^J \pi_j \mathcal{N}(\mathbf{x} | \mu_j, \Sigma_j), \quad (1)$$

where  $\mathbf{x}, \Theta$  represent the points and GMMs parameters respectively.  $\Theta$  consists of  $J$  triplets  $(\pi_j, \mu_j, \Sigma_j)$ , where  $\pi_j$  is a scalar mixture weight and  $\sum_j \pi_j = 1$ ,  $\mu_j \in \mathbb{R}^{3 \times 1}$  is the mean vector and  $\Sigma_j \in \mathbb{R}^{3 \times 3}$  is the covariance matrix of the  $j$ -th component.

For filtering out the outliers, simply using bi-directional first nearest nei matching can lead to plenty of misjudgements, due to the randomness of the probabilistic model. We loose the strict rules by only removing the GMMs which

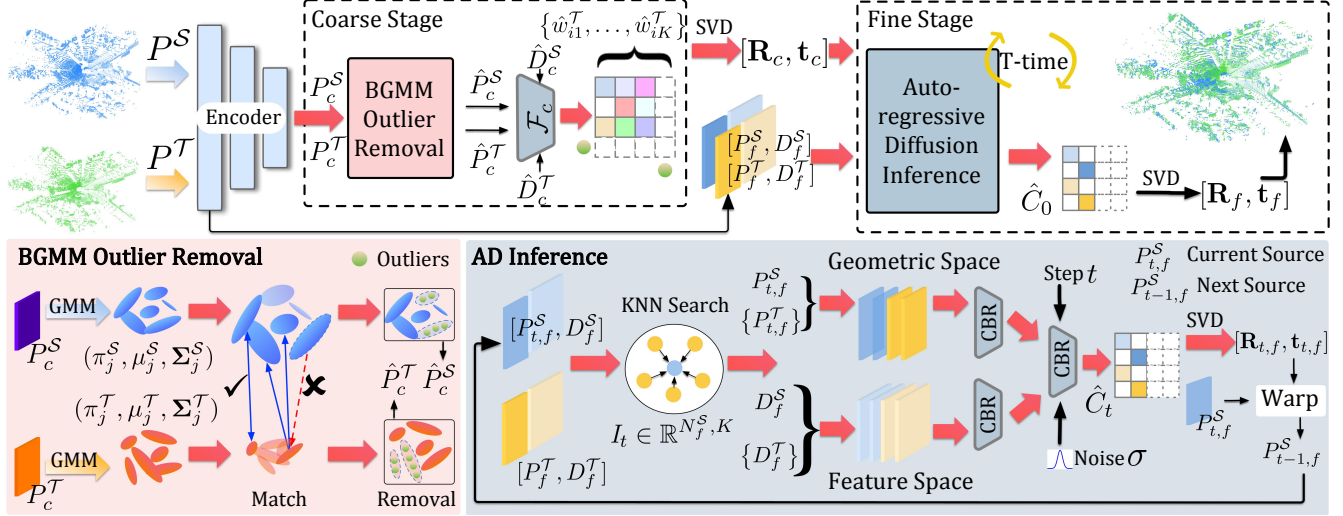


Figure 2. The detector-descriptor backbone hierarchically downsamples the input point cloud pairs and extracts corresponding features. Next, the BGMM Outlier Removal module purifies the input points and leverages the predictor network  $\mathcal{F}_c$  along with SVD to perform coarse registration. Finally, our proposed AD inference framework autoregressively generates regional correspondences and predicts the final registration result.

is not the top-K neighbor of its nearest counterpart as:

$$\mathcal{G}_{out}^S = \{\Theta_i^S \in \Theta^S \mid \Theta_i^S \notin N_k(\Theta_j^T), \Theta_j^T = N_1(\Theta_i^S)\}. \quad (2)$$

After obtaining the outlier GMMs, we can filter out the attached outlier points  $p_{i,c}^S \in \mathcal{G}_{out}^S$ , where the purified points are denoted as  $\hat{p}_{i,c}^S$ . The outlier GMMs  $\mathcal{G}_{out}^T$  and the purified points  $\hat{p}_{i,c}^T$  are computed in the same way. Several removal results are presented in Sec. 4.

Based on the purified point clouds  $\hat{p}_{i,c}^S, \hat{p}_{i,c}^T$ , we can further predict the truly P2P correspondence for coarse registration. Firstly, We perform KNN search on the feature space  $\hat{d}_i^S$  to retrieve the top-K nearest candidates  $\{\hat{d}_{i1}^T, \dots, \hat{d}_{iK}^T\}$ , their corresponding geometric points  $\{\hat{p}_{i1}^T, \dots, \hat{p}_{iK}^T\}$ , and uncertainty value  $\{\hat{u}_{i1}^T, \dots, \hat{u}_{iK}^T\}$ . We can firstly construct their geometric features as:

$$F_G = [\hat{p}_c^S, \{\hat{p}_c^T\}, p_c^S - \{\hat{p}_c^T\}, \|p_c^S - \{\hat{p}_c^T\}\|_2], \quad (3)$$

where  $[\cdot]$  denotes the concatenation operation and  $\{\cdot\}$  denotes the candidates group. By introducing the cosine similarity function, we can also measure the similarity between the source features and their top-K nearest neighbors as:

$$S_{ij} = \frac{\langle \hat{d}_i^S, \hat{d}_j^T \rangle}{\|\hat{d}_i^S\|_2 \|\hat{d}_j^T\|_2}, (i \in \hat{N}_c^S, j \in iK) \quad (4)$$

The descriptor features can be constructed as:

$$F_D = [\hat{d}_c^S, \{\hat{d}_c^T\}, \hat{u}_c^S, \{\hat{u}_c^T\}, S] \quad (5)$$

Then the confidence scores for each candidate is predicted by the prediction network  $\mathcal{F}_c$  as:

$$\{\hat{w}_{i1}^T, \dots, \hat{w}_{iK}^T\}_{i \in \hat{N}_c^S} = \text{Softmax}(\mathcal{F}_c[F_G, F_D]) \quad (6)$$

Where  $\hat{w}_{ij}^T$  denotes the similarity of the top-j neighborhood with  $\hat{p}_{i,c}^S$ .

We can use the weighted sum operation to generate the counterpart of  $\hat{p}_{i,c}^S$

$$\hat{p}_{i,c}^{fuse} = \sum_{k=1}^K \hat{w}_{ik}^T \hat{p}_{ik}^T \quad (7)$$

We also obtain the fused features  $\hat{d}_i^{fuse}$  in the same way and utilize MLP layers to predict the confidence weights for coarse registration

$$\hat{w}_i = \text{MLP}(\hat{d}_i^{fuse}) \quad (8)$$

The coarse transformation  $\mathbf{R}_c, \mathbf{t}_c$  can be calculated through the Weighted SVD decomposition:

$$\mathbf{R}_c, \mathbf{t}_c = \min_{\mathbf{R}, \mathbf{t}} \sum \hat{w}_i \|\mathbf{R} \cdot \hat{p}_{i,c}^S + \mathbf{t} - \hat{p}_{i,c}^{fuse}\|_2^2 \quad (9)$$

### 3.3. Efficient Autoregressive Diffusion

Previous correspondence-based registration methods [47, 58, 63] focus on directly generating the global P2P correspondence with dimension  $N^S \times N^T$ . However, the diffusion-based methods are roundly criticized for the low convergence speed, predicting global dense P2P correspondences will aggravate the burden of training computation as

in the Sec.4.3, especially for large-scale scenes. To tackle this problem, we observe that the top-K neighbors searching in source frame are effective enough to find accurate correspondences for each point in target frame, based on the reliable coarse registration results.

**Diffusion Correspondence:** In this paper, we formulate the correspondence generation as a denoising process  $p_\theta(C_{t-1}|C_t, \mathbf{c})$ . Specifically, a neural network  $\mathcal{F}_f(C_t, t, F_G, F_D)$  is designed by taking the geometric features  $F_G$  and descriptor features  $F_D$  as conditions, where the intermediate correspondence is denoted as  $C_t \in \mathbb{R}^{N_f^S \times K}$ . Finally, the output distribution of  $\tilde{C}_0 \in \mathbb{R}^{N_f^S \times K}$  is generated progressively through the denoising process.

Specifically, source points  $p_{i,t,f}^S$ , firstly retrieve their top-K nearest candidates  $\{p_{i1}^T, \dots, p_{iK}^T\}$ , corresponding descriptors  $\{d_{i1}^T, \dots, d_{iK}^T\}$  and uncertainty values  $\{u_{i1}^T, \dots, u_{iK}^T\}$ . Similar to the coarse stage, the geometric features can be constructed as:

$$F_G^t = [p_{i,t,f}^S, \{p_{i,f}^T\}, p_{i,f}^S - \{p_{i,f}^T\}, \|p_{i,f}^S - \{p_{i,f}^T\}\|_2]. \quad (10)$$

Take computational overhead into consideration, in the fine stage, we no longer calculate the similarities, the descriptor features can be constructed as:

$$F_D = [d_f^S, \{d_f^T\}, u_f^S, \{u_f^T\}]. \quad (11)$$

Finally, by fusing the features with the noisy correspondence  $C_t$  and the time  $t$ , we can get the denoised correspondence  $\tilde{C}_0$  through  $\mathcal{F}_f[C_t, t, F_G^t, F_D]$ .

**Autoregressive Inference:** Inspired by diffusion-based temporal motion prediction methods [1, 51, 53], we rethink the diffusion-based PCR as a autoregressive process. During inference, the diffusion model will generate robust point correspondence matrix between adjacent two adjacent sampling steps. The generated correspondences are then decomposed into translation and rotation to warp the input source points, which will constitute the next step's source point. Specifically, obtaining the denoised correspondence from  $\mathcal{F}_f$ , we can perform the Softmax operation on the correspondence  $\tilde{C}_0$  to get the similarity towards top-K candidates of  $p_{i,t,f}^S$  as:

$$\{w_{i1}^T, \dots, w_{iK}^T\}_{i \in N_f^S} = \text{Softmax}(\mathcal{F}_f[C_t, t, F_G^t, F_D]). \quad (12)$$

Similar to Eq. 7, 8 and 9, the transformation matrix  $\{(\mathbf{R}_{t-1,f}, \mathbf{t}_{t-1,f}) \mid t \in T\}$  can be derived as:

$$\mathbf{R}_{t-1,f}, \mathbf{t}_{t-1,f} = \arg \min_{\mathbf{R}, \mathbf{t}} \sum_i^{N_S} w_{i,t} \left\| \mathbf{R} p_{i,t,f}^S + \mathbf{t} - p_{i,t,f}^{fuse} \right\|_2, \quad (13)$$

Where  $p_{i,t,f}^S$  denotes the source point warped by the current transformation as:

$$p_{i,t,f}^S = \tilde{\mathbf{R}}_{t-1,f} p_{i,f}^S + \tilde{\mathbf{t}}_{t-1,f}. \quad (14)$$

The transformation  $\{\tilde{\mathbf{Tr}}_{t-1} = (\tilde{\mathbf{R}}_{t-1}, \tilde{\mathbf{t}}_{t-1})\}$  is built on the previous transformation history as:

$$\tilde{\mathbf{Tr}}_{t-1} = \prod_{i=T}^{t-1} \mathbf{Tr}_i, \tilde{\mathbf{Tr}}_T = \mathbf{Tr}_T = \mathbf{Tr}_c. \quad (15)$$

Since the transformation is derived from the denoised correspondence, we can formulate the autoregressive inference paradigm as:

$$p(C^T, \dots, C^t) = \prod_t p(C^t \mid C^T, \dots, C^{t-1}). \quad (16)$$

In this case, the prediction of the correspondence is based on the correspondence history, which fulfills the general form of autoregression. We refer to this inference manner as Autoregressively Inference.

### 3.4. Loss Function

The overall loss function can be written as:

$$\mathcal{L} = \mathcal{L}_{\text{trans}} + \alpha \mathcal{L}_{\text{rot}} + \mathcal{L}_{\text{diff}}, \quad (17)$$

where  $\mathcal{L}_{\text{trans}}$  and  $\mathcal{L}_{\text{rot}}$  are translation loss and rotation loss, respectively.  $\mathcal{L}_{\text{diff}}$  is the loss in diffusion model training. Specifically, given each estimated transformation in the forward process  $\tilde{\mathbf{R}}, \tilde{\mathbf{t}}$  and the ground truth  $\mathbf{R}, \mathbf{t}$ ,  $\mathcal{L}_{\text{trans}}$  and  $\mathcal{L}_{\text{rot}}$  can be calculated as:

$$\mathcal{L}_{\text{trans}} = \|\mathbf{t} - \tilde{\mathbf{t}}\|_2, l \in \{c, f\}, \quad (18)$$

$$\mathcal{L}_{\text{rot}} = \left\| \tilde{\mathbf{R}}^T \mathbf{R}_l - \mathbf{I} \right\|_2, l \in \{c, f\}, \quad (19)$$

where  $\mathbf{I}$  denotes identity matrix. The training loss for the diffusion model  $\mu_f$  is presented as:

$$\mathcal{L}_{\text{diff}} = \mathbb{E}_{t \sim [0, T]} \|\mathcal{F}_f[C_t, t, F_G^t, F_D] - C_{gt}\|^2. \quad (20)$$

In order to get the supervision  $C_{gt}$ , we first use the GT transformation  $\mathbf{R}, \mathbf{t}$  to warp the source superpoints as  $P_{gt}^S = \mathbf{R} P^S + \mathbf{t}$ . Then, we obtain the global correspondence matrix  $\tilde{C}_{gt}$  by utilizing the Optimal Transport algorithm [54] to refine the distance matrix between  $P_{gt}^S$  and  $P^T$ . Finally, each source superpoint  $P_{gt}^S$  searches its  $K$  nearest target superpoints  $P^T$  to build the local GT corresponding  $C_{gt} \in \mathbb{R}^{N_f^S \times K}$ .

## 4. Experiments

### 4.1. Datasets and Implementation Details

**Datasets.** We conduct extensive experiments on three large-scale point cloud datasets, KITTI [15], NuScenes [3] and Apollo [40]. KITTI odometry dataset consists of 11 sequences (00-10) with ground truth vehicles poses. It is worth noting that, in the outdoor PCR field, the point cloud

Table 1. Registration performance on KITTI dataset and NuScenes dataset.

Methods	KITTI dataset				NuScenes dataset			
	RTE (m) ↓	RRE (deg) ↓	Recall ↑	Time (ms) ↓	RTE (m) ↓	RRE (deg) ↓	Recall ↑	Time (ms) ↓
ICP[2]	0.04 ± 0.05	0.11 ± 0.09	14.3%	472.2	0.25 ± 0.51	0.25 ± 0.50	18.8%	82.0
FGR[67]	0.93 ± 0.59	0.96 ± 0.81	39.4%	506.1	0.71 ± 0.62	1.01 ± 0.92	32.2%	284.6
RANSAC[13]	0.13 ± 0.07	0.54 ± 0.40	91.9%	549.6	0.21 ± 0.19	0.74 ± 0.70	60.9%	268.2
DCP[57]	1.03 ± 0.51	2.07 ± 1.19	47.3%	46.4	1.09 ± 0.49	2.07 ± 1.14	58.6%	45.5
IDAM[28]	0.66 ± 0.48	1.06 ± 0.94	70.9%	33.4	0.47 ± 0.41	0.79 ± 0.78	88.0%	32.6
FMR[22]	0.66 ± 0.42	1.49 ± 0.85	90.6%	85.5	0.60 ± 0.39	1.61 ± 0.97	92.1%	61.1
DGR[8]	0.32 ± 0.32	0.37 ± 0.30	98.7%	1496.6	0.21 ± 0.18	0.48 ± 0.43	98.4%	523.0
RegFormer[32]	0.08 ± 0.11	0.23 ± 0.21	99.8%	98.3	0.20 ± --	0.22 ± --	99.9%	85.6
HRegNet[39]	0.047 ± 0.037	0.147 ± 0.120	100%	136.0	0.110 ± 0.096	0.285 ± 0.209	100%	120.1
HDMNet[62]	0.050 ± 0.057	0.159 ± 0.152	99.85%	120.2	0.114 ± 0.102	0.274 ± 0.206	100%	102.9
FlyCore[30]	0.05 ± --	0.28 ± --	99.7%	154	0.17 ± --	0.32 ± --	99.7%	128
EADReg	<b>0.040 ± 0.035</b>	<b>0.116 ± 0.096</b>	<b>100%</b>	129.4	<b>0.090 ± 0.072</b>	<b>0.248 ± 0.187</b>	<b>100%</b>	112.4

**Algorithm 1** EADReg: Autogressive Inference

**Require:** Registration  $\mathbf{R}_c, \mathbf{t}_c$  from the coarse stage; Point clouds  $P_f^S \in \mathbb{R}^{N_f^S \times 3}, P_f^T \in \mathbb{R}^{N_f^T \times 3}$  and corresponding descriptors  $D_f^S, D_f^T$  with uncertainty values  $U_f^S, U_f^T$ .

**Target:** the denoised correspondence  $\hat{C}_0 \in \mathbb{R}^{N_f^S \times K}$ .

- 1:  $C_T \sim \mathcal{N}(0, 1)^{N \times M}$
- 2:  $P_{T,f}^S = \mathbf{R}_c P_f^S + \mathbf{t}_c \rightarrow F_G^T$
- 3:  $F_D = [D_f^S, \{D_f^T\}, U_f^S, \{U_f^T\}]$
- 4: **for**  $t = T, \dots, 1$  **do**
- 5:    $\hat{C}_0 \leftarrow \mathcal{F}_f[C_t, t, F_G^t, F_D]$
- 6:    $\mathbf{Tr}_{t-1} \leftarrow \mathbf{R}_{t-1,f}, \mathbf{t}_{t-1,f} \leftarrow \hat{C}_0$    ▷ Equation (7,8,12,13)
- 7:    $\tilde{\mathbf{Tr}}_{t-1} = \prod_{i=T}^{t-1} \mathbf{Tr}_i, \tilde{\mathbf{Tr}}_0 = \mathbf{Tr}_0 = \mathbf{R}_c$
- 8:    $P_{t-1,f}^S = \tilde{\mathbf{R}}_{t-1,f} P_f^S + \tilde{\mathbf{t}}_{t-1,f} \rightarrow F_G^{t-1}$
- 9:    $\epsilon_t \leftarrow \frac{\hat{C}_0 - \sqrt{\alpha_t} \hat{C}_t}{\sqrt{1 - \alpha_t}}$
- 10:    $\hat{C}_{t-1} \leftarrow \sqrt{\alpha_{t-1}} \hat{C}_0 + \sqrt{1 - \alpha_{t-1} - \sigma_t^2} \epsilon_t + \sigma_t z_t$
- 11: **end for**

pairs we used for training, validation and testing are point clouds between a certain interval frame. The interval is set to 10 as in [32, 39]. Additionally, the metrics of the indoor methods like Geotransformer [47] is different from ours, for fair comparison we only consider outdoor PCR methods.

According to the settings of the KITTI dataset in [32, 39], sequences 00-05 are used for training, sequences 06-07 for validation and sequences 08-10 for testing. NuScenes dataset comprises 1000 scenes, and we use the first 700 scenes for training, the following 150 scenes for validation, and the last 150 for testing. The Apollo-SouthBay dataset contains six routes, where we choose five of them except SunnyvaleBigloop route, to conduct fair experimental comparison following [39].

**Implementation Details** We first utilize voxelization for

downsampling, the voxel size is set to 0.3m. After that, we randomly sample 16384 points in the KITTI and Apollo datasets and 8192 points in the NuScenes dataset for registration. Our testing procedure for all experiments utilizes DDIM [49] for acceleration, and the influence of different sampling steps will be discussed in the Sec.. The learning rate is initially set to 0.001 with a weight decay of 50% every 10 epochs. The training framework is implemented with PyTorch 2.0.1 and Adam optimizer. For training procedure, we first utilize chamfer [27] and match loss [38] to pretrain our detector-descriptor backbone for robust feature extraction, then train the entire model with batch size 16 for 50 epochs iterations on a single node with an NVIDIA GeForce 3090 GPU with Intel Xeon W-2265 CPU.

**4.2. Evaluation**

**Qualitative Visualization** We visualize the registration results with 3 samples from KITTI, Nuscenes and Apollo datasets in Fig.3.

Specifically, we first select the correspondences with confidence weights  $\hat{w}$  greater than 0.001. Then, we warp the selected source points using the ground truth transformation. If the distance between a warped source point and the target point exceeds 5 meters, the correspondence is considered a wrong prediction; otherwise, it is regarded as correct.

To verify the effectiveness of our proposed BGMM Outlier Removal module, we present four removal results in Fig. 4. From the visualization, it is evident that BGMM successfully removes outlier points and retains all the points relevant for registration.

**Quantitative Evaluation** We adopt relative translation error (RTE), relative rotation error (RRE), registration recall (RR) and average running time on the test point cloud pairs to evaluate the registration performance. Specifically, since the failed registrations can result in exceptionally large RRE and RTE values, leading to unreliable error metrics [39].

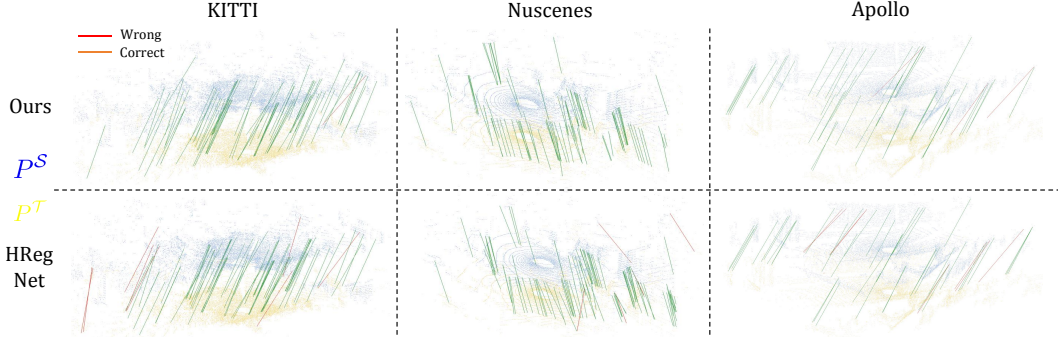


Figure 3. Qualitative visualization of registration performance. From left to right, we compare our proposed method with HRegNet using three samples from the KITTI, NuScenes, and Apollo-Southbay datasets, respectively. Specifically, we select only the correspondences with confidence weights  $\hat{w}$  greater than 0.001.

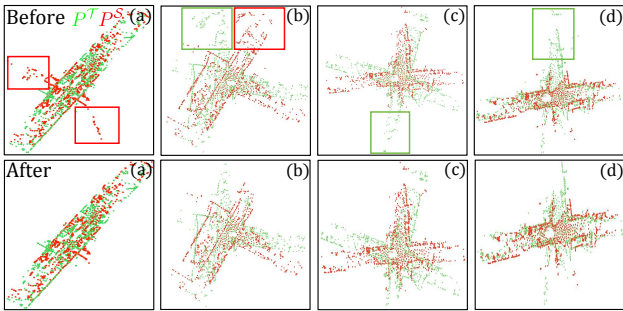


Figure 4. We select four samples from the KITTI dataset to illustrate the outlier removal process using the BGMM module. The first row contains the original point clouds, and the second row shows the purified version. The outliers are framed within boxes.

Table 2. Registration Performance on Apollo-Southbay Dataset

Model	RTE (m) ↓	RRE (deg) ↓	Recall ↑	Time (ms) ↓
ICP[2]	0.039 ± 0.170	0.046 ± 0.257	46.45%	470.2
RANSAC[13]	0.125 ± 0.114	0.361 ± 0.308	83.72%	552.1
DCP[57]	1.174 ± 0.499	2.155 ± 1.254	28.49%	41.0
IDAM[28]	0.456 ± 0.116	0.127 ± 0.429	24.03%	32.0
FMR[22]	0.653 ± 0.188	0.727 ± 0.658	83.76%	83.4
DGR[8]	0.132 ± 0.151	0.127 ± 0.146	99.64%	257.0
HRegNet[39]	0.034 ± 0.037	0.079 ± 0.079	99.88%	129.5
EADReg	<b>0.028 ± 0.031</b>	<b>0.064 ± 0.062</b>	<b>99.92%</b>	121.6

We define successful registration as occurring when both the Relative Translation Error (RTE) and the Relative Rotation Error (RRE) fall within the thresholds  $RTE < 2m$  and  $RRE < 5^\circ$ , respectively. The registration performance of different methods are presented in Tab. 1.

**Comparison with baseline methods:** We choose ICP [2], RANSAC [13] and Fast Global Registration (FGR) [67] as on behalf of the classical PCR methods, as for learning-based methods, we select DCP [57], IDAM [28], FMR [22], DGR [8], RegFormer [32], HRegNet [39], HDMNet [62] and Flycore [30] for comparison.

According to the results in Tab. 1, classical methods either achieve poor recall performance on KITTI and Nuscenes datasets (with 14.25% and 39.42% for ICP and FGR on KITTI respectively), or generate suboptimal transformation compared with Learning-based methods (with average RTE 0.929 and 0.126 for FGR and RANSAC respectively). Moreover, since classical methods require iterative optimization for convergence, learning based methods present better efficiency.

With the development of the learning-based PCR methods, the recall presents a significant upward trend, and start with RegFormer the recall achieve nearly 100% on both KITTI and Nuscenes datasets under the generally outdoor PCR setting. Specifically, Although the DCP, IDAM, and FMR exhibit significantly lower inference times compared to EADReg, the EADReg shows notably higher average RTE and RRE values. RegFormer, HRegNet, HDMNet and Flycore both achieve centimetre-level RTE performance on KITTI dataset, with 0.08, 0.047, 0.05 and 0.05 respectively. Our proposed EADReg outperforms all the baselines and achieve 0.040 average RTE and 0.117 RRE degree, exceeding HRegNet by 0.7cm and 0.03 degree.

Meanwhile, on Nuscenes dataset, EADReg is the only one reaches centimetre-level RTE performance, exceeding HRegNet and RegFormer by 2cm and 11cm respectively. Meanwhile, the variance of EADReg is the smallest across KITTI and Nuscenes, with 3.5cm and 7.2cm respectively.

Additionally, EADReg does not suffer from the slow inference problem commonly associated with diffusion-based models. In fact, the running time of EADReg is faster than FlyCore and HRegNet by 22.8 ms and 4.8 ms, respectively, effectively demonstrating the efficiency of EADReg.

**Comparison on Apollo-Southbay dataset:** Apollo-Southbay dataset has 35109 test data samples and is about six times bigger than KITTI and Nuscenes. Therefore, the results on the Apollo dataset can more accurately reflect the model’s performance.

Table 3. Ablation studies of the architecture.

Model	RTE (m)	RRE (deg)	Recall	Time (ms)
Only Coarse	0.119 ± 0.102	0.373 ± 0.284	99.97%	95.5
EADReg w/o GMM	0.042 ± 0.035	0.143 ± 0.118	100%	113.5
<b>EADReg</b>	<b>0.040 ± 0.034</b>	<b>0.117 ± 0.107</b>	<b>100.00%</b>	129.4

Table 4. Ablation study results of EADReg on the GMM outlier rejection with different number of clusters  $J$ . The best results for each criterion are labeled in bold.

Clusters	RTE (m)	RRE (deg)	Recall	Time (ms)
$J = 8$	0.040 ± 0.034	<b>0.116 ± 0.096</b>	100.00%	<b>129.4</b>
$J = 12$	0.041 ± 0.035	0.117 ± 0.094	100.00%	136.2
$J = 16$	<b>0.039 ± 0.036</b>	0.115 ± 0.101	100.00%	140.8
$J = 32$	0.042 ± 0.039	0.123 ± 0.110	99.96%	143.5

Table 5. Ablation study results of the hyperparameter  $\alpha$ 's influence on the registration results on KITTI dataset. The best results for each criterion are labeled in bold.

$\alpha$	RTE (m)	RRE (deg)	Recall
$\alpha = 1$	0.041 ± 0.038	0.154 ± 0.122	99.99%
$\alpha = 2$	0.040 ± 0.036	0.133 ± 0.111	100.00%
$\alpha = 3$	0.042 ± 0.036	0.121 ± 0.103	100.00%
$\alpha = 4$	<b>0.040 ± 0.035</b>	0.116 ± 0.096	100%
$\alpha = 5$	0.041 ± 0.039	0.116 ± 0.100	99.99%
$\alpha = 6$	0.043 ± 0.038	<b>0.100 ± 0.089</b>	99.97%

Refer to Tab.2, EADReg achieves the best performance compared with the baseline methods, surpasses the suboptimal method HRegNet on the average RTE, average RRE and recall with 0.6cm, 0.015 degree and 0.04% respectively, the variants of EADReg on RTE and RRE are also the smallest, with 3.1cm and 0.06 degree.

Based on comprehensive experiments, it is evident that the newly introduced EADReg surpasses existing methods in terms of accuracy and successfully strikes a favorable balance between performance and efficiency.

### 4.3. Ablation Study

We perform abundant ablation studies on KITTI dataset to demonstrate the effectiveness of the hierarchical structure and the introduction of the similarity features.

**Network Structure:** We use the output transformation  $\mathbf{R}$ ,  $\mathbf{t}$  from the coarse stage and the fine stage respectively for evaluation. The registration results are shown in Tab.3. Since the average RRE of the coarse stage with 0.119cm is better than the learning based method DGR [8] with 0.32, we can demonstrate that the coarse stage do provide a reliable initial transformation.

**Number of GMM Clusters:** According to the results in Tab. 4, although the results show minimal changes as  $J$  increases, the inference time increases steadily, from 129.4 ms to 143.5 ms. Thus, we choose  $J = 8$  for experiments.

Table 6. Ablation study results of EADReg with different scale of correspondence region  $K$ , Occ is the abbreviation of the GPU memory occupancy during training.

$K$	RTE (m)	RRE (deg)	Recall	Time (ms)	Occ (MB)
$K = 1$	0.042 ± 0.039	0.122 ± 0.114	100.100%	128.7	19083
$K = 3$	<b>0.040 ± 0.034</b>	<b>0.117 ± 0.107</b>	100.00%	129.4	20583
$K = 5$	0.041 ± 0.035	0.116 ± 0.106	99.99%	131.4	22033
$K = 7$	0.041 ± 0.035	0.122 ± 0.102	100.100%	132.2	23571

Table 7. Ablation study results of EADReg with different sampling steps.

$K$	RTE (m)	RRE (deg)	Recall	Time (ms)
$S = 1$	0.048 ± 0.040	0.132 ± 0.111	99.99%	115.6
$S = 2$	0.0418 ± 0.035	0.118 ± 0.098	99.99%	123.2
$S = 3$	0.040 ± 0.034	0.116 ± 0.096	100.00%	129.4
$S = 4$	0.040 ± 0.033	0.115 ± 0.096	99.99%	136.2
$S = 5$	0.040 ± 0.033	0.115 ± 0.097	99.99%	141.2
$S = 6$	0.040 ± 0.033	0.114 ± 0.098	99.99%	148.8

**Weight of the  $\alpha$ :** EADReg is trained with combinations of translation loss  $\mathcal{L}_{trans}$ , rotation loss  $\alpha\mathcal{L}_{rot}$  and diffusion loss  $\mathcal{L}_{diff}$ . We leave the ablation study of different set the weights of  $\mathcal{L}_{diff}$  and  $\mathcal{L}_{trans}$  to 1 for experiments and leave the ablation study in the supplementary materials. According to Tab.5, as the  $\alpha$  increases, the average RRE monotonically decreases from 0.154 to 0.100 and RTE reaches the best when  $\alpha = 4$ . In order to balance the performance between RTE and RRE metrics, we choose  $\alpha = 4$  for our experiments, which achieves the best RTE with 4cm and suboptimal RRE with 0.115 degree, and the best recall 100%.

**Number of Correspondence Candidate:** In this part, we demonstrate the reason why generating the global P2P correspondence  $C \in \mathbb{R}^{N_f^S \times N^T}$  can be impractical for deployment. From Table 6, we observe that increasing  $K$  only slightly affects registration performance, supporting our hypothesis that true correspondences lie in the nearest top-K neighbors after reliable coarse registration. However, GPU memory usage rises sharply from 19,083 MB to 23,571 MB, indicating that predicting global P2P correspondences will inevitably lead to prohibitive training overhead.

**Number of Sampling Steps:** We further conduct several experiments with different diffusion step numbers and present the results in Tab.7. We observe that the performance stabilize after  $S = 3$ , and shows minor improvements when  $S > 3$ . Meanwhile, the inference time of EADReg monotonically increasing, from 115.6ms to 148.8ms, in order to balance the accuracy and efficiency, we choose  $S = 3$  in our method.

## 5. Conclusion

In this paper, we provide an efficient diffusion-based network for large-scale outdoor LiDAR point cloud registra-



tion named EADReg. EADReg follows a coarse-to-fine registration paradigm, which leverages detector-descriptor backbone to downsample the original point cloud and extract the corresponding features. In the coarse stage, we propose the BGMM module to reject the outlier points. In the fine stage, we introduce autogressive diffusion inference to generate the reliable P2P correspondence. Extensive experiments show that EADReg achieves a favourable balance between performance and efficiency.

## References

- [1] German Barquero, Sergio Escalera, and Cristina Palmero. Belfusion: Latent diffusion for behavior-driven human motion prediction. In *2023 IEEE/CVF International Conference on Computer Vision (ICCV)*, page 2317–2327. IEEE, 2023. 2, 3, 5
- [2] Paul J Besl and Neil D McKay. Method for registration of 3-d shapes. In *Sensor fusion IV: control paradigms and data structures*, pages 586–606. Spie, 1992. 2, 6, 7
- [3] Holger Caesar, Varun Bankiti, Alex H Lang, Sourabh Vora, Venice Erin Liong, Qiang Xu, Anush Krishnan, Yu Pan, Giancarlo Baldan, and Oscar Beijbom. nuscenes: A multi-modal dataset for autonomous driving. In *Proceedings of the IEEE/CVF conference on computer vision and pattern recognition*, pages 11621–11631, 2020. 5
- [4] Daniele Cattaneo, Matteo Vaghi, and Abhinav Valada. Lcd-net: Deep loop closure detection and point cloud registration for lidar slam. *IEEE Transactions on Robotics*, 38(4): 2074–2093, 2022. 1
- [5] Guangyan Chen, Meiling Wang, Li Yuan, Yi Yang, and Yufeng Yue. Rethinking point cloud registration as masking and reconstruction. In *2023 IEEE/CVF International Conference on Computer Vision (ICCV)*, page 17671–17681. IEEE, 2023. 2, 3
- [6] Zhilei Chen, Honghua Chen, Lina Gong, Xuefeng Yan, Jun Wang, Yanwen Guo, Jing Qin, and Mingqiang Wei. Utopic: Uncertainty-aware overlap prediction network for partial point cloud registration. *Computer Graphics Forum*, 41(7):87–98, 2022. 2, 3
- [7] Zhi Chen, Yufan Ren, Tong Zhang, Zheng Dang, Wenbing Tao, Sabine Süsstrunk, and Mathieu Salzmann. Diffusion-pcr: Diffusion models for robust multi-step point cloud registration. *arXiv preprint arXiv:2312.03053*, 2023. 1, 2, 3
- [8] Christopher Choy, Wei Dong, and Vladlen Koltun. Deep global registration. In *Proceedings of the IEEE/CVF conference on computer vision and pattern recognition*, pages 2514–2523, 2020. 6, 7, 8
- [9] Arthur P Dempster, Nan M Laird, and Donald B Rubin. Maximum likelihood from incomplete data via the em algorithm. *Journal of the royal statistical society: series B (methodological)*, 39(1):1–22, 1977. 3
- [10] Zhongying Deng, Yanqi Chen, Lihao Liu, Shujun Wang, Rihuan Ke, Carola-Bibiane Schonlieb, and Angelica I Aviles-Rivero. Trafficcam: A versatile dataset for traffic flow segmentation. *arXiv preprint arXiv:2211.09620*, 2022. 1
- [11] Gil Elbaz, Tamar Avraham, and Anath Fischer. 3d point cloud registration for localization using a deep neural network auto-encoder. In *2017 IEEE Conference on Computer Vision and Pattern Recognition (CVPR)*. IEEE, 2017. 1
- [12] Georgios D Evangelidis, Dionyssos Kounades-Bastian, Radu Horaud, and Emmanouil Z Psarakis. A generative model for the joint registration of multiple point sets. In *European conference on computer vision*, pages 109–122. Springer, 2014. 3
- [13] Martin A Fischler and Robert C Bolles. Random sample consensus: a paradigm for model fitting with applications to image analysis and automated cartography. *Communications of the ACM*, 24(6):381–395, 1981. 2, 6, 7
- [14] Wei Gao and Russ Tedrake. Filterreg: Robust and efficient probabilistic point-set registration using gaussian filter and twist parameterization. In *Proceedings of the IEEE/CVF conference on computer vision and pattern recognition*, pages 11095–11104, 2019. 3
- [15] Andreas Geiger, Philip Lenz, and Raquel Urtasun. Are we ready for autonomous driving? the kitti vision benchmark suite. In *2012 IEEE conference on computer vision and pattern recognition*, pages 3354–3361. IEEE, 2012. 5
- [16] Bo Han, Hao Peng, Minjing Dong, Yi Ren, Yixuan Shen, and Chang Xu. Amd: Autoregressive motion diffusion. In *Proceedings of the AAAI Conference on Artificial Intelligence*, pages 2022–2030, 2024. 3
- [17] Eric Hedlin, Gopal Sharma, Shweta Mahajan, Hossam Isack, Abhishek Kar, Andrea Tagliasacchi, and Kwang Moo Yi. Unsupervised semantic correspondence using stable diffusion. *Advances in Neural Information Processing Systems*, 36, 2024. 3
- [18] Thomas Hitchcox and James Richard Forbes. A point cloud registration pipeline using gaussian process regression for bathymetric slam. In *2020 IEEE/RSJ International Conference on Intelligent Robots and Systems (IROS)*. IEEE, 2020. 1
- [19] Jonathan Ho, Ajay Jain, and Pieter Abbeel. Denoising diffusion probabilistic models. *Advances in Neural Information Processing Systems*, 33:6840–6851, 2020. 3
- [20] Jonathan Ho, William Chan, Chitwan Saharia, Jay Whang, Ruiqi Gao, Alexey Gritsenko, Diederik P Kingma, Ben Poole, Mohammad Norouzi, David J Fleet, et al. Imagen video: High definition video generation with diffusion models. *arXiv preprint arXiv:2210.02303*, 2022. 2
- [21] Emiel Hoogeboom, Alexey A Gritsenko, Jasmijn Bastings, Ben Poole, Rianne van den Berg, and Tim Salimans. Autoregressive diffusion models. *arXiv preprint arXiv:2110.02037*, 2021. 3
- [22] Xiaoshui Huang, Guofeng Mei, and Jian Zhang. Feature-metric registration: A fast semi-supervised approach for robust point cloud registration without correspondences. In *2020 IEEE/CVF Conference on Computer Vision and Pattern Recognition (CVPR)*. IEEE, 2020. 6, 7
- [23] Chiyu “Max” Jiang, Andre Cornman, Cheolho Park, Benjamin Sapp, Yin Zhou, and Dragomir Anguelov. Motioidfuser: Controllable multi-agent motion prediction using diffusion. In *2023 IEEE/CVF Conference on Computer Vision and Pattern Recognition (CVPR)*. IEEE, 2023. 2

- [24] Haobo Jiang, Mathieu Salzmann, Zheng Dang, Jin Xie, and Jian Yang. Se3diffusion model-based point cloud registration for robust 6d object pose estimation. *Advances in Neural Information Processing Systems*, 36, 2024. 2, 3
- [25] Saike Jiang, Peng Qi, Leng Han, Limin Liu, Yangfan Li, Zhan Huang, Yajia Liu, and Xiongkui He. Navigation system for orchard spraying robot based on 3d lidar slam with ndt-icp point cloud registration. 2023. 1
- [26] Pileun Kim, Jisoo Park, Yong K. Cho, and Junsuk Kang. Uav-assisted autonomous mobile robot navigation for as-is 3d data collection and registration in cluttered environments. *Automation in Construction*, 106:102918, 2019. 1
- [27] Jiaxin Li and Gim Hee Lee. Usip: Unsupervised stable interest point detection from 3d point clouds. In *Proceedings of the IEEE/CVF international conference on computer vision*, pages 361–370, 2019. 6
- [28] Jiahao Li, Changhao Zhang, Ziyao Xu, Hangning Zhou, and Chi Zhang. Iterative distance-aware similarity matrix convolution with mutual-supervised point elimination for efficient point cloud registration. In *Computer Vision—ECCV 2020: 16th European Conference, Glasgow, UK, August 23–28, 2020, Proceedings, Part XXIV 16*, pages 378–394. Springer, 2020. 6, 7
- [29] Yang Li and Tatsuya Harada. Leopard: Learning partial point cloud matching in rigid and deformable scenes. In *2022 IEEE/CVF Conference on Computer Vision and Pattern Recognition (CVPR)*. IEEE, 2022. 2
- [30] Zikuan Li, Kaijun Zhang, Zhoutao Wang, Sibowu, Xiaoping Zhang, Mingqiang Wei, and Jun Wang. Flycore: Fast low-frequency coarse registration of large-scale outdoor lidar point clouds. *IEEE Transactions on Geoscience and Remote Sensing*, 2024. 6, 7
- [31] Jiuming Liu, Guangming Wang, Chaokang Jiang, Zhe Liu, and Hesheng Wang. Translo: A window-based masked point transformer framework for large-scale lidar odometry. In *Proceedings of the AAAI Conference on Artificial Intelligence*, pages 1683–1691, 2023. 1
- [32] Jiuming Liu, Guangming Wang, Zhe Liu, Chaokang Jiang, Marc Pollefeys, and Hesheng Wang. Regformer: An efficient projection-aware transformer network for large-scale point cloud registration. In *Proceedings of the IEEE/CVF International Conference on Computer Vision*, pages 8451–8460, 2023. 2, 6, 7
- [33] Jiuming Liu, Jinru Han, Lihao Liu, Angelica I Aviles-Rivero, Chaokang Jiang, Zhe Liu, and Hesheng Wang. Mamba4d: Efficient long-sequence point cloud video understanding with disentangled spatial-temporal state space models. *arXiv preprint arXiv:2405.14338*, 2024. 1
- [34] Jiuming Liu, Guangming Wang, Weicai Ye, Chaokang Jiang, Jinru Han, Zhe Liu, Guofeng Zhang, Dalong Du, and Hesheng Wang. DiffFlow3d: Toward robust uncertainty-aware scene flow estimation with iterative diffusion-based refinement. In *Proceedings of the IEEE/CVF Conference on Computer Vision and Pattern Recognition*, pages 15109–15119, 2024. 1
- [35] Jiuming Liu, Dong Zhuo, Zhiheng Feng, Siting Zhu, Chen-sheng Peng, Zhe Liu, and Hesheng Wang. Dvlo: Deep visual-lidar odometry with local-to-global feature fusion and bi-directional structure alignment. In *European Conference on Computer Vision*, pages 475–493. Springer, 2025. 1
- [36] Lihao Liu, Angelica I Aviles-Rivero, and Carola-Bibiane Schönlieb. Contrastive registration for unsupervised medical image segmentation. *IEEE Transactions on Neural Networks and Learning Systems*, 2023. 2
- [37] Lihao Liu, Yanqi Cheng, Dongdong Chen, Jing He, Pietro Liò, Carola-Bibiane Schönlieb, and Angelica I Aviles-Rivero. Traffic video object detection using motion prior. *arXiv preprint arXiv:2311.10092*, 2023. 2
- [38] Fan Lu, Guang Chen, Yinlong Liu, Zhongnan Qu, and Alois Knoll. Rskdd-net: Random sample-based keypoint detector and descriptor. *Advances in Neural Information Processing Systems*, 33:21297–21308, 2020. 6
- [39] Fan Lu, Guang Chen, Yinlong Liu, Lijun Zhang, Sanqing Qu, Shu Liu, Rongqi Gu, and Changjun Jiang. Hregnet: A hierarchical network for efficient and accurate outdoor lidar point cloud registration. *IEEE Transactions on Pattern Analysis and Machine Intelligence*, 45(10):11884–11897, 2023. 2, 3, 6, 7
- [40] Weixin Lu, Yao Zhou, Guowei Wan, Shenhua Hou, and Shiyu Song. L3-net: Towards learning based lidar localization for autonomous driving. In *Proceedings of the IEEE/CVF Conference on Computer Vision and Pattern Recognition*, pages 6389–6398, 2019. 5
- [41] Grace Luo, Lisa Dunlap, Dong Huk Park, Aleksander Holynski, and Trevor Darrell. Diffusion hyperfeatures: Searching through time and space for semantic correspondence. *Advances in Neural Information Processing Systems*, 36, 2024. 3
- [42] Yanzi Miao, Yang Liu, Hongbin Ma, and Huijie Jin. The pose estimation of mobile robot based on improved point cloud registration. *International Journal of Advanced Robotic Systems*, 13(2):52, 2016. 1
- [43] Jisu Nam, Gyuseong Lee, Sunwoo Kim, Hyeonsu Kim, Hyungwon Cho, Seyeon Kim, and Seungryong Kim. Diffusion model for dense matching. In *The Twelfth International Conference on Learning Representations*. 2, 3
- [44] François Pomerleau, Francis Colas, and Roland Siegwart. *A Review of Point Cloud Registration Algorithms for Mobile Robotics*. now Publishers Inc, 2015. 1
- [45] Charles R Qi, Hao Su, Kaichun Mo, and Leonidas J Guibas. Pointnet: Deep learning on point sets for 3d classification and segmentation. In *Proceedings of the IEEE conference on computer vision and pattern recognition*, pages 652–660, 2017. 2
- [46] Zhijian Qiao, Zehuan Yu, Binqian Jiang, Huan Yin, and Shaojie Shen. G3reg: Pyramid graph-based global registration using gaussian ellipsoid model. *IEEE Transactions on Automation Science and Engineering*, 2024. 3
- [47] Zheng Qin, Hao Yu, Changjian Wang, Yulan Guo, Yuxing Peng, Slobodan Ilic, Dewen Hu, and Kai Xu. Geotransformer: Fast and robust point cloud registration with geometric transformer. *IEEE Transactions on Pattern Analysis and Machine Intelligence*, 45(8):9806–9821, 2023. 1, 2, 4, 6
- [48] Rui She, Qiyu Kang, Sijie Wang, Wee Peng Tay, Kai Zhao, Yang Song, Tianyu Geng, Yi Xu, Diego Navarro Navarro,

- and Andreas Hartmannsgruber. Pointdifformer: Robust point cloud registration with neural diffusion and transformer. *IEEE Transactions on Geoscience and Remote Sensing*, 2024. 2, 3
- [49] Jiaming Song, Chenlin Meng, and Stefano Ermon. Denoising diffusion implicit models. 2020. 6
- [50] Lei Sun. Practical, fast and robust point cloud registration for scene stitching and object localization. *IEEE Access*, 10: 3962–3978, 2022. 1
- [51] Bowen Tang, Kaihao Zhang, Wenhan Luo, Wei Liu, and Hongdong Li. *Prompting Future Driven Diffusion Model for Hand Motion Prediction*, page 169–186. Springer Nature Switzerland, 2024. 2, 3, 5
- [52] Hugues Thomas, Charles R. Qi, Jean-Emmanuel Deschaud, Beatriz Marcotegui, Francois Goulette, and Leonidas Guibas. Kpconv: Flexible and deformable convolution for point clouds. In *2019 IEEE/CVF International Conference on Computer Vision (ICCV)*. IEEE, 2019. 2
- [53] Tom Van Wouwe, Seunghwan Lee, Antoine Falisse, Scott Delp, and C. Karen Liu. Diffusionposer: Real-time human motion reconstruction from arbitrary sparse sensors using autoregressive diffusion. In *2024 IEEE/CVF Conference on Computer Vision and Pattern Recognition (CVPR)*, page 2513–2523. IEEE, 2024. 2, 3, 5
- [54] Cédric Villani et al. *Optimal transport: old and new*. Springer, 2009. 5
- [55] Haiping Wang, Yuan Liu, Qingyong Hu, Bing Wang, Jianguo Chen, Zhen Dong, Yulan Guo, Wenping Wang, and Bisheng Yang. Roreg: Pairwise point cloud registration with oriented descriptors and local rotations. *IEEE Transactions on Pattern Analysis and Machine Intelligence*, 45(8):10376–10393, 2023. 2
- [56] Jianyuan Wang, Christian Rupprecht, and David Novotny. Posediffusion: Solving pose estimation via diffusion-aided bundle adjustment. In *Proceedings of the IEEE/CVF International Conference on Computer Vision*, pages 9773–9783, 2023. 3
- [57] Yue Wang and Justin Solomon. Deep closest point: Learning representations for point cloud registration. In *2019 IEEE/CVF International Conference on Computer Vision (ICCV)*. IEEE, 2019. 6, 7
- [58] Qianliang Wu, Haobo Jiang, Yaqing Ding, Lei Luo, Jin Xie, and Jian Yang. Diff-pcr: Diffusion-based correspondence searching in doubly stochastic matrix space for point cloud registration. *arXiv preprint arXiv:2401.00436*, 2023. 2, 3, 4
- [59] Tong Wu, Zhihao Fan, Xiao Liu, Hai-Tao Zheng, Yeyun Gong, Jian Jiao, Juntao Li, Jian Guo, Nan Duan, Weizhu Chen, et al. Ar-diffusion: Auto-regressive diffusion model for text generation. *Advances in Neural Information Processing Systems*, 36:39957–39974, 2023. 3
- [60] Qian Xie, Yiming Zhang, Xuanming Cao, Yabin Xu, Dening Lu, HongHua Chen, and Jun Wang. Part-in-whole point cloud registration for aircraft partial scan automated localization. *Computer-Aided Design*, 137:103042, 2021. 1
- [61] Hao Xu, Shuaicheng Liu, Guangfu Wang, Guanghui Liu, and Bing Zeng. Omnet: Learning overlapping mask for partial-to-partial point cloud registration. In *2021 IEEE/CVF International Conference on Computer Vision (ICCV)*, page 3112–3121. IEEE, 2021. 2, 3
- [62] Weiyi Xue, Fan Lu, and Guang Chen. Hdmnet: A hierarchical matching network with double attention for large-scale outdoor lidar point cloud registration. In *Proceedings of the IEEE/CVF Winter Conference on Applications of Computer Vision*, pages 3393–3403, 2024. 6, 7
- [63] Hao Yu, Fu Li, Mahdi Saleh, Benjamin Busam, and Slobodan Ilic. Cofinet: Reliable coarse-to-fine correspondences for robust pointcloud registration. *Advances in Neural Information Processing Systems*, 34:23872–23884, 2021. 4
- [64] Wentao Yuan, Benjamin Eckart, Kihwan Kim, Varun Jampani, Dieter Fox, and Jan Kautz. Deepgmr: Learning latent gaussian mixture models for registration. In *Computer Vision—ECCV 2020: 16th European Conference, Glasgow, UK, August 23–28, 2020, Proceedings, Part V 16*, pages 733–750. Springer, 2020. 2, 3
- [65] Mingyuan Zhang, Xinying Guo, Liang Pan, Zhongang Cai, Fangzhou Hong, Huirong Li, Lei Yang, and Ziwei Liu. Remodiffuse: Retrieval-augmented motion diffusion model. In *2023 IEEE/CVF International Conference on Computer Vision (ICCV)*. IEEE, 2023. 2
- [66] Hengshuang Zhao, Li Jiang, Jiaya Jia, Philip HS Torr, and Vladlen Koltun. Point transformer. In *Proceedings of the IEEE/CVF international conference on computer vision*, pages 16259–16268, 2021. 2
- [67] Qian-Yi Zhou, Jaesik Park, and Vladlen Koltun. Fast global registration. In *Computer Vision—ECCV 2016: 14th European Conference, Amsterdam, The Netherlands, October 11–14, 2016, Proceedings, Part II 14*, pages 766–782. Springer, 2016. 6, 7
- [68] Yao Zhou, Guowei Wan, Shenhua Hou, Li Yu, Gang Wang, Xiaofei Rui, and Shiyu Song. Da4ad: End-to-end deep attention-based visual localization for autonomous driving. In *Computer Vision—ECCV 2020: 16th European Conference, Glasgow, UK, August 23–28, 2020, Proceedings, Part XXVIII 16*, pages 271–289. Springer, 2020. 3
- [69] Jing Zou, Noémie Debroux, Lihao Liu, Jing Qin, Carola-Bibiane Schönlieb, and Angelica I Aviles-Rivero. Learning homeomorphic image registration via conformal-invariant hyperelastic regularisation. *arXiv preprint arXiv:2303.08113*, 2023. 1

## References

- [1] German Barquero, Sergio Escalera, and Cristina Palmero. Belfusion: Latent diffusion for behavior-driven human motion prediction. In *2023 IEEE/CVF International Conference on Computer Vision (ICCV)*, page 2317–2327. IEEE, 2023. 2, 3, 5
- [2] Paul J Besl and Neil D McKay. Method for registration of 3-d shapes. In *Sensor fusion IV: control paradigms and data structures*, pages 586–606. Spie, 1992. 2, 6, 7
- [3] Holger Caesar, Varun Bankiti, Alex H Lang, Sourabh Vora, Venice Erin Liong, Qiang Xu, Anush Krishnan, Yu Pan, Giancarlo Baldan, and Oscar Beijbom. nuscenes: A multi-modal dataset for autonomous driving. In *Proceedings of*

- the *IEEE/CVF conference on computer vision and pattern recognition*, pages 11621–11631, 2020. 5
- [4] Daniele Cattaneo, Matteo Vaghi, and Abhinav Valada. Lcdnet: Deep loop closure detection and point cloud registration for lidar slam. *IEEE Transactions on Robotics*, 38(4): 2074–2093, 2022. 1
- [5] Guangyan Chen, Meiling Wang, Li Yuan, Yi Yang, and Yufeng Yue. Rethinking point cloud registration as masking and reconstruction. In *2023 IEEE/CVF International Conference on Computer Vision (ICCV)*, page 17671–17681. IEEE, 2023. 2, 3
- [6] Zhilei Chen, Honghua Chen, Lina Gong, Xuefeng Yan, Jun Wang, Yanwen Guo, Jing Qin, and Mingqiang Wei. Utopic: Uncertainty-aware overlap prediction network for partial point cloud registration. *Computer Graphics Forum*, 41(7):87–98, 2022. 2, 3
- [7] Zhi Chen, Yufan Ren, Tong Zhang, Zheng Dang, Wenbing Tao, Sabine Süsstrunk, and Mathieu Salzmann. Diffusion-pcr: Diffusion models for robust multi-step point cloud registration. *arXiv preprint arXiv:2312.03053*, 2023. 1, 2, 3
- [8] Christopher Choy, Wei Dong, and Vladlen Koltun. Deep global registration. In *Proceedings of the IEEE/CVF conference on computer vision and pattern recognition*, pages 2514–2523, 2020. 6, 7, 8
- [9] Arthur P Dempster, Nan M Laird, and Donald B Rubin. Maximum likelihood from incomplete data via the em algorithm. *Journal of the royal statistical society: series B (methodological)*, 39(1):1–22, 1977. 3
- [10] Zhongying Deng, Yanqi Chen, Lihao Liu, Shujun Wang, Rihuan Ke, Carola-Bibiane Schonlieb, and Angelica I Aviles-Rivero. Trafficcam: A versatile dataset for traffic flow segmentation. *arXiv preprint arXiv:2211.09620*, 2022. 1
- [11] Gil Elbaz, Tamar Avraham, and Anath Fischer. 3d point cloud registration for localization using a deep neural network auto-encoder. In *2017 IEEE Conference on Computer Vision and Pattern Recognition (CVPR)*. IEEE, 2017. 1
- [12] Georgios D Evangelidis, Dionyssos Kounades-Bastian, Radu Horaud, and Emmanouil Z Psarakis. A generative model for the joint registration of multiple point sets. In *European conference on computer vision*, pages 109–122. Springer, 2014. 3
- [13] Martin A Fischler and Robert C Bolles. Random sample consensus: a paradigm for model fitting with applications to image analysis and automated cartography. *Communications of the ACM*, 24(6):381–395, 1981. 2, 6, 7
- [14] Wei Gao and Russ Tedrake. Filterreg: Robust and efficient probabilistic point-set registration using gaussian filter and twist parameterization. In *Proceedings of the IEEE/CVF conference on computer vision and pattern recognition*, pages 11095–11104, 2019. 3
- [15] Andreas Geiger, Philip Lenz, and Raquel Urtasun. Are we ready for autonomous driving? the kitti vision benchmark suite. In *2012 IEEE conference on computer vision and pattern recognition*, pages 3354–3361. IEEE, 2012. 5
- [16] Bo Han, Hao Peng, Minjing Dong, Yi Ren, Yixuan Shen, and Chang Xu. Amd: Autoregressive motion diffusion. In *Proceedings of the AAAI Conference on Artificial Intelligence*, pages 2022–2030, 2024. 3
- [17] Eric Hedlin, Gopal Sharma, Shweta Mahajan, Hossam Isack, Abhishek Kar, Andrea Tagliasacchi, and Kwang Moo Yi. Unsupervised semantic correspondence using stable diffusion. *Advances in Neural Information Processing Systems*, 36, 2024. 3
- [18] Thomas Hitchcox and James Richard Forbes. A point cloud registration pipeline using gaussian process regression for bathymetric slam. In *2020 IEEE/RSJ International Conference on Intelligent Robots and Systems (IROS)*. IEEE, 2020. 1
- [19] Jonathan Ho, Ajay Jain, and Pieter Abbeel. Denoising diffusion probabilistic models. *Advances in Neural Information Processing Systems*, 33:6840–6851, 2020. 3
- [20] Jonathan Ho, William Chan, Chitwan Saharia, Jay Whang, Ruiqi Gao, Alexey Gritsenko, Diederik P Kingma, Ben Poole, Mohammad Norouzi, David J Fleet, et al. Imagen video: High definition video generation with diffusion models. *arXiv preprint arXiv:2210.02303*, 2022. 2
- [21] Emiel Hoogeboom, Alexey A Gritsenko, Jasmijn Bastings, Ben Poole, Rianne van den Berg, and Tim Salimans. Autoregressive diffusion models. *arXiv preprint arXiv:2110.02037*, 2021. 3
- [22] Xiaoshui Huang, Guofeng Mei, and Jian Zhang. Feature-metric registration: A fast semi-supervised approach for robust point cloud registration without correspondences. In *2020 IEEE/CVF Conference on Computer Vision and Pattern Recognition (CVPR)*. IEEE, 2020. 6, 7
- [23] Chiyu “Max” Jiang, Andre Cornman, Cheolho Park, Benjamin Sapp, Yin Zhou, and Dragomir Anguelov. Motioidiffuser: Controllable multi-agent motion prediction using diffusion. In *2023 IEEE/CVF Conference on Computer Vision and Pattern Recognition (CVPR)*. IEEE, 2023. 2
- [24] Haobo Jiang, Mathieu Salzmann, Zheng Dang, Jin Xie, and Jian Yang. Se3diffusion model-based point cloud registration for robust 6d object pose estimation. *Advances in Neural Information Processing Systems*, 36, 2024. 2, 3
- [25] Saike Jiang, Peng Qi, Leng Han, Limin Liu, Yangfan Li, Zhan Huang, Yajia Liu, and Xiongkui He. Navigation system for orchard spraying robot based on 3d lidar slam with ndt-icp point cloud registration. 2023. 1
- [26] Pileun Kim, Jisoo Park, Yong K. Cho, and Junsuk Kang. Uav-assisted autonomous mobile robot navigation for as-is 3d data collection and registration in cluttered environments. *Automation in Construction*, 106:102918, 2019. 1
- [27] Jiaxin Li and Gim Hee Lee. Usip: Unsupervised stable interest point detection from 3d point clouds. In *Proceedings of the IEEE/CVF international conference on computer vision*, pages 361–370, 2019. 6
- [28] Jiahao Li, Changhao Zhang, Ziyao Xu, Hangning Zhou, and Chi Zhang. Iterative distance-aware similarity matrix convolution with mutual-supervised point elimination for efficient point cloud registration. In *Computer Vision—ECCV 2020: 16th European Conference, Glasgow, UK, August 23–28, 2020, Proceedings, Part XXIV 16*, pages 378–394. Springer, 2020. 6, 7
- [29] Yang Li and Tatsuya Harada. Leopard: Learning partial point cloud matching in rigid and deformable scenes. In

- 2022 *IEEE/CVF Conference on Computer Vision and Pattern Recognition (CVPR)*. IEEE, 2022. 2
- [30] Zikuan Li, Kaijun Zhang, Zhoutao Wang, Sibow Wu, Xiaoping Zhang, Mingqiang Wei, and Jun Wang. Flycore: Fast low-frequency coarse registration of large-scale outdoor lidar point clouds. *IEEE Transactions on Geoscience and Remote Sensing*, 2024. 6, 7
- [31] Jiuming Liu, Guangming Wang, Chaokang Jiang, Zhe Liu, and Hesheng Wang. Translo: A window-based masked point transformer framework for large-scale lidar odometry. In *Proceedings of the AAAI Conference on Artificial Intelligence*, pages 1683–1691, 2023. 1
- [32] Jiuming Liu, Guangming Wang, Zhe Liu, Chaokang Jiang, Marc Pollefeys, and Hesheng Wang. Regformer: An efficient projection-aware transformer network for large-scale point cloud registration. In *Proceedings of the IEEE/CVF International Conference on Computer Vision*, pages 8451–8460, 2023. 2, 6, 7
- [33] Jiuming Liu, Jinru Han, Lihao Liu, Angelica I Aviles-Rivero, Chaokang Jiang, Zhe Liu, and Hesheng Wang. Mamba4d: Efficient long-sequence point cloud video understanding with disentangled spatial-temporal state space models. *arXiv preprint arXiv:2405.14338*, 2024. 1
- [34] Jiuming Liu, Guangming Wang, Weicai Ye, Chaokang Jiang, Jinru Han, Zhe Liu, Guofeng Zhang, Dalong Du, and Hesheng Wang. Diffflow3d: Toward robust uncertainty-aware scene flow estimation with iterative diffusion-based refinement. In *Proceedings of the IEEE/CVF Conference on Computer Vision and Pattern Recognition*, pages 15109–15119, 2024. 1
- [35] Jiuming Liu, Dong Zhuo, Zhiheng Feng, Siting Zhu, Chen-sheng Peng, Zhe Liu, and Hesheng Wang. Dvlo: Deep visual-lidar odometry with local-to-global feature fusion and bi-directional structure alignment. In *European Conference on Computer Vision*, pages 475–493. Springer, 2025. 1
- [36] Lihao Liu, Angelica I Aviles-Rivero, and Carola-Bibiane Schönlieb. Contrastive registration for unsupervised medical image segmentation. *IEEE Transactions on Neural Networks and Learning Systems*, 2023. 2
- [37] Lihao Liu, Yanqi Cheng, Dongdong Chen, Jing He, Pietro Liò, Carola-Bibiane Schönlieb, and Angelica I Aviles-Rivero. Traffic video object detection using motion prior. *arXiv preprint arXiv:2311.10092*, 2023. 2
- [38] Fan Lu, Guang Chen, Yinlong Liu, Zhongnan Qu, and Alois Knoll. Rskdd-net: Random sample-based keypoint detector and descriptor. *Advances in Neural Information Processing Systems*, 33:21297–21308, 2020. 6
- [39] Fan Lu, Guang Chen, Yinlong Liu, Lijun Zhang, Sanqing Qu, Shu Liu, Rongqi Gu, and Changjun Jiang. Hregnet: A hierarchical network for efficient and accurate outdoor lidar point cloud registration. *IEEE Transactions on Pattern Analysis and Machine Intelligence*, 45(10):11884–11897, 2023. 2, 3, 6, 7
- [40] Weixin Lu, Yao Zhou, Guowei Wan, Shenhua Hou, and Shiyu Song. L3-net: Towards learning based lidar localization for autonomous driving. In *Proceedings of the IEEE/CVF Conference on Computer Vision and Pattern Recognition*, pages 6389–6398, 2019. 5
- [41] Grace Luo, Lisa Dunlap, Dong Huk Park, Aleksander Holynski, and Trevor Darrell. Diffusion hyperfeatures: Searching through time and space for semantic correspondence. *Advances in Neural Information Processing Systems*, 36, 2024. 3
- [42] Yanzi Miao, Yang Liu, Hongbin Ma, and Huijie Jin. The pose estimation of mobile robot based on improved point cloud registration. *International Journal of Advanced Robotic Systems*, 13(2):52, 2016. 1
- [43] Jisu Nam, Gyuseong Lee, Sunwoo Kim, Hyeonsu Kim, Hyoungwon Cho, Seyeon Kim, and Seungryong Kim. Diffusion model for dense matching. In *The Twelfth International Conference on Learning Representations*. 2, 3
- [44] François Pomerleau, Francis Colas, and Roland Siegwart. *A Review of Point Cloud Registration Algorithms for Mobile Robotics*. now Publishers Inc, 2015. 1
- [45] Charles R Qi, Hao Su, Kaichun Mo, and Leonidas J Guibas. Pointnet: Deep learning on point sets for 3d classification and segmentation. In *Proceedings of the IEEE conference on computer vision and pattern recognition*, pages 652–660, 2017. 2
- [46] Zhijian Qiao, Zehuan Yu, Binqian Jiang, Huan Yin, and Shaojie Shen. G3reg: Pyramid graph-based global registration using gaussian ellipsoid model. *IEEE Transactions on Automation Science and Engineering*, 2024. 3
- [47] Zheng Qin, Hao Yu, Changjian Wang, Yulan Guo, Yuxing Peng, Slobodan Ilic, Dewen Hu, and Kai Xu. Geotransformer: Fast and robust point cloud registration with geometric transformer. *IEEE Transactions on Pattern Analysis and Machine Intelligence*, 45(8):9806–9821, 2023. 1, 2, 4, 6
- [48] Rui She, Qiyu Kang, Sijie Wang, Wee Peng Tay, Kai Zhao, Yang Song, Tianyu Geng, Yi Xu, Diego Navarro Navarro, and Andreas Hartmannsgruber. Pointdiffuser: Robust point cloud registration with neural diffusion and transformer. *IEEE Transactions on Geoscience and Remote Sensing*, 2024. 2, 3
- [49] Jiaming Song, Chenlin Meng, and Stefano Ermon. Denoising diffusion implicit models. 2020. 6
- [50] Lei Sun. Practical, fast and robust point cloud registration for scene stitching and object localization. *IEEE Access*, 10: 3962–3978, 2022. 1
- [51] Bowen Tang, Kaihao Zhang, Wenhan Luo, Wei Liu, and Hongdong Li. *Prompting Future Driven Diffusion Model for Hand Motion Prediction*, page 169–186. Springer Nature Switzerland, 2024. 2, 3, 5
- [52] Hugues Thomas, Charles R. Qi, Jean-Emmanuel Deschaud, Beatriz Marcotequi, Francois Goulette, and Leonidas Guibas. Kpconv: Flexible and deformable convolution for point clouds. In *2019 IEEE/CVF International Conference on Computer Vision (ICCV)*. IEEE, 2019. 2
- [53] Tom Van Wouwe, Seunghwan Lee, Antoine Falisse, Scott Delp, and C. Karen Liu. Diffusionposer: Real-time human motion reconstruction from arbitrary sparse sensors using autoregressive diffusion. In *2024 IEEE/CVF Conference on Computer Vision and Pattern Recognition (CVPR)*, page 2513–2523. IEEE, 2024. 2, 3, 5
- [54] Cédric Villani et al. *Optimal transport: old and new*. Springer, 2009. 5

- [55] Haiping Wang, Yuan Liu, Qingyong Hu, Bing Wang, Jianguo Chen, Zhen Dong, Yulan Guo, Wenping Wang, and Bisheng Yang. Roreg: Pairwise point cloud registration with oriented descriptors and local rotations. *IEEE Transactions on Pattern Analysis and Machine Intelligence*, 45(8):10376–10393, 2023. 2
- [56] Jianyuan Wang, Christian Rupprecht, and David Novotny. Posediffusion: Solving pose estimation via diffusion-aided bundle adjustment. In *Proceedings of the IEEE/CVF International Conference on Computer Vision*, pages 9773–9783, 2023. 3
- [57] Yue Wang and Justin Solomon. Deep closest point: Learning representations for point cloud registration. In *2019 IEEE/CVF International Conference on Computer Vision (ICCV)*. IEEE, 2019. 6, 7
- [58] Qianliang Wu, Haobo Jiang, Yaqing Ding, Lei Luo, Jin Xie, and Jian Yang. Diff-pcr: Diffusion-based correspondence searching in doubly stochastic matrix space for point cloud registration. *arXiv preprint arXiv:2401.00436*, 2023. 2, 3, 4
- [59] Tong Wu, Zhihao Fan, Xiao Liu, Hai-Tao Zheng, Yeyun Gong, Jian Jiao, Juntao Li, Jian Guo, Nan Duan, Weizhu Chen, et al. Ar-diffusion: Auto-regressive diffusion model for text generation. *Advances in Neural Information Processing Systems*, 36:39957–39974, 2023. 3
- [60] Qian Xie, Yiming Zhang, Xuanming Cao, Yabin Xu, Dening Lu, HongHua Chen, and Jun Wang. Part-in-whole point cloud registration for aircraft partial scan automated localization. *Computer-Aided Design*, 137:103042, 2021. 1
- [61] Hao Xu, Shuaicheng Liu, Guangfu Wang, Guanghui Liu, and Bing Zeng. Omnet: Learning overlapping mask for partial-to-partial point cloud registration. In *2021 IEEE/CVF International Conference on Computer Vision (ICCV)*, page 3112–3121. IEEE, 2021. 2, 3
- [62] Weiyi Xue, Fan Lu, and Guang Chen. Hdmnet: A hierarchical matching network with double attention for large-scale outdoor lidar point cloud registration. In *Proceedings of the IEEE/CVF Winter Conference on Applications of Computer Vision*, pages 3393–3403, 2024. 6, 7
- [63] Hao Yu, Fu Li, Mahdi Saleh, Benjamin Busam, and Slobodan Ilic. Cofinet: Reliable coarse-to-fine correspondences for robust pointcloud registration. *Advances in Neural Information Processing Systems*, 34:23872–23884, 2021. 4
- [64] Wentao Yuan, Benjamin Eckart, Kihwan Kim, Varun Jampani, Dieter Fox, and Jan Kautz. Deepgmr: Learning latent gaussian mixture models for registration. In *Computer Vision–ECCV 2020: 16th European Conference, Glasgow, UK, August 23–28, 2020, Proceedings, Part V 16*, pages 733–750. Springer, 2020. 2, 3
- [65] Mingyuan Zhang, Xinying Guo, Liang Pan, Zhongang Cai, Fangzhou Hong, Huirong Li, Lei Yang, and Ziwei Liu. Remodiffuse: Retrieval-augmented motion diffusion model. In *2023 IEEE/CVF International Conference on Computer Vision (ICCV)*. IEEE, 2023. 2
- [66] Hengshuang Zhao, Li Jiang, Jiaya Jia, Philip HS Torr, and Vladlen Koltun. Point transformer. In *Proceedings of the IEEE/CVF international conference on computer vision*, pages 16259–16268, 2021. 2
- [67] Qian-Yi Zhou, Jaesik Park, and Vladlen Koltun. Fast global registration. In *Computer Vision–ECCV 2016: 14th European Conference, Amsterdam, The Netherlands, October 11–14, 2016, Proceedings, Part II 14*, pages 766–782. Springer, 2016. 6, 7
- [68] Yao Zhou, Guowei Wan, Shenhua Hou, Li Yu, Gang Wang, Xiaofei Rui, and Shiyu Song. Da4ad: End-to-end deep attention-based visual localization for autonomous driving. In *Computer Vision–ECCV 2020: 16th European Conference, Glasgow, UK, August 23–28, 2020, Proceedings, Part XXVIII 16*, pages 271–289. Springer, 2020. 3
- [69] Jing Zou, Noémie Debroux, Lihao Liu, Jing Qin, Carola-Bibiane Schönlieb, and Angelica I Aviles-Rivero. Learning homeomorphic image registration via conformal-invariant hyperelastic regularisation. *arXiv preprint arXiv:2303.08113*, 2023. 1